

GALOPP: Multi-Agent Deep Reinforcement Learning For Persistent Monitoring With Localization Constraints

Manav Mishra, Prithvi Poddar, Jingxi Chen, P.B. Sujit and Pratap Tokekar

Abstract—Persistently monitoring a region under localization and communication constraints is a challenging problem. In this paper, we consider a heterogeneous robotic system consisting of two types of agents – anchor agents that have accurate localization capability, and auxiliary agents that have low localization accuracy. The auxiliary agents must be within the communication range of an anchor, directly or indirectly to localize itself. The objective of the robotic team is to minimize the uncertainty in the environment through persistent monitoring. We propose a multi-agent deep reinforcement learning (MADRL) based architecture with graph attention called Graph Localized Proximal Policy Optimization (GALOPP), which incorporates the localization and communication constraints of the agents along with persistent monitoring objective to determine motion policies for each agent. We evaluate the performance of GALOPP on three different custom-built environments. The results show the agents are able to learn a stable policy and outperform greedy and random search baseline approaches.

I. INTRODUCTION

Visibility-based Persistent Monitoring (PM) problem involves the continuous surveillance of a bounded environment by a system of robots [1]–[6]. Several applications like search and rescue, border patrol, critical infrastructure, etc. require persistent monitoring to obtain timely information. We study the problem of planning trajectories for each agent in a multi-robot system for persistently monitoring an environment. When the environment becomes increasingly complex, it becomes challenging to monitor using any deterministic coordinating strategies for PM [6]. Therefore, there is a need for developing strategies for the agents that can learn on how to navigate in such environments. One such approach is to use Multi-Agent Deep Reinforcement Learning (MADRL) algorithms to determine the policies for the individual agents to navigate in the environment [7].

In this paper, we consider a scenario where a team of multiple robots equipped with a limited field-of-view (FOV) sensor are deployed to monitor a GPS-denied environment as shown in Figure 1. We assume the environment does not support GPS and hence one can deploy agents with high accuracy Inertial Measurement Unit (IMU) like Honeywell-HG1700 [8], that can enable the agents to accurately localize. However, the cost of high accuracy IMU is in tens of thousands of dollars and hence the operation becomes highly expensive. On the other hand, we can use low cost IMU

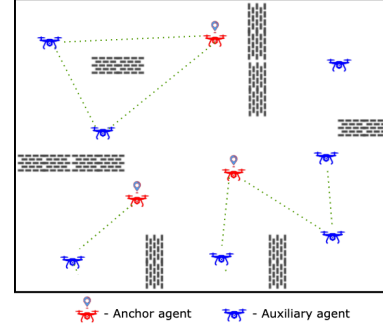


Fig. 1: Persistent monitoring using anchor and auxiliary agents with FOV, localization and communication range constraint.

for the agents, however they are subject to drift resulting in poor localization. Therefore, we consider two types of localization agents in the team – anchor and auxiliary agents. The anchor agents have high accuracy IMU and hence can localize accurately by themselves (with very low position uncertainty). However, auxiliary agents have low accuracy IMU and require periodic measurements from the anchor agents to update their position. The auxiliary agents use the notion of cooperative localization [9]–[11] to localize by communicating with the anchor agents directly or indirectly through other auxiliary agents and hence have uncertainty in their positional beliefs. Further, the agents have finite communication range which restricts the auxiliary agents motion [12] and hence the agents may not be able to monitor the complete region as any communication disconnection from the anchor agents will result in poor localization and hence affects the coverage accuracy. However, intermittent disconnection will enable the agents to recover from the localization uncertainty and also cover regions. This conflicting objective of monitoring the complete area while periodically maintaining connectivity from the anchor agents makes the problem of determining persistent monitoring strategies for the agents challenging.

In this paper, we propose a MADRL with graph attention based architecture called the Graph Localized Proximal Policy Optimization (GALOPP) to perform persistent monitoring with such heterogeneous agents subject to localization and communication constraints. As the agents have communication constraints which also affects the localization of the auxiliary agents, the graph attention based architecture effectively facilitates checks for agent-to-agent connectivity as they perform surveillance of the environment.

Manav Mishra, Prithvi Poddar and P.B. Sujit are with Department of Electrical Engineering and Computer Science, IISER Bhopal, Bhopal, India – 462038.

Jingxi Chen and Pratap Tokekar are with the Department of Computer Science, University of Maryland, Baltimore, United States.

For persistent monitoring, the environment is modelled as a two-dimensional discrete grid. Each cell in the grid is allocated a penalty. When a cell is within the sensing range of any agent then the penalty value reduces to zero, otherwise the penalty accumulates over time. Thus, the agents must learn their motion strategy such that the net penalty accumulated over a time period is minimized which shows efficient persistent monitoring.

The main contribution of the paper is the MADRL graph attention based architecture GALOPP that determines policies for the agents taking the localization and communication constraints and the robot heterogeneity into account. To validate the performance of the GALOPP, we develop a custom environment for the simulation and compare the performance of GALOPP against random and greedy baseline strategies.

II. RELATED WORK

In the literature, persistent monitoring and cooperative localization have been addressed as individual topics of interest and there are inadequate works that consider these two aspects jointly. The mobile variant of the Art Gallery Problem (AGP) [13] details the goal is to determine the upper bound on the minimum number of agents required for patrolling the path/segments so as to minimize the time taken to cover the entire area. The objective of the Watchman Route Problem (WRP) [14] is to find the minimum length trajectory for a watchman (robot) to cover every point inside the input polygon. In addition, there have been several deterministic variants of multi-robot planning algorithms within the environment [1], [2], [5], [15]. In general, the deterministic visibility coverage problems are NP-hard and can provide an approximation of the optimal solution. However, these approaches determine static policies which do not take communication and localization constraints into account and hence cannot be directly used in the current problem.

MADRL based approaches have been proposed for studies on cooperative multi-agent tasks covering a wide spectrum of applications [16]–[21]. In [16] inter-agent communication for self-interested agents is studied for cooperative path planning, but they assume complete connectivity throughout without factoring in localization constraints. In [17], the notion of MARL under partial observability was formalized. The proposed scenario is also partially observable as the agents have limited sensing range. In [7], a method to find the trajectories for each agent to continuously cover the area is developed. However the agents do not have communication and localization constraints. In [21], a message-aware attention mechanism has been proposed that assigns relative importance to the messages received for coverage application. However, persistence monitoring with localization constraints introduces higher complexity which is addressed in this paper compared to [21].

For determining coordination strategies, it is essential for robots to incorporate the positional beliefs of surrounding agents and obstacles. Previously, there have been several works describing methods to achieve cooperative localization under limited inter-vehicle connectivity [9], [10], [22]–[24].

We incorporate the idea of cooperative localization using Kalman Filter to achieve localization for the auxiliary agent.

III. PROBLEM STATEMENT

A. Formal description of PM

We consider the PM problem for a 2D grid world $G \subseteq \mathbb{R}^2$ of size $M \times N$. Each grid cell $G_{\alpha\beta}$, $1 \leq \alpha \leq M$ and $1 \leq \beta \leq N$, has a reward $R_{\alpha\beta}(t)$ associated with it at time t . When the cell $G_{\alpha\beta}$ is within the sensing range of an agent, then $R_{\alpha\beta}(t) \leftarrow 0$, otherwise, the reward decays with a decay parameter $\Delta_{\alpha\beta} > 0$ until it reaches a minimum value of $-R_{\max}$. We consider negative reward as it refers to penalty on the cell for not monitoring. At time $t = 0$, $R_{\alpha\beta}(t) = 0$, $\forall(\alpha, \beta)$ and $R_{\alpha\beta}(t+1) = \max\{R_{\alpha\beta}(t) - \Delta_{\alpha\beta}, -R_{\max}\}$ if $G_{\alpha\beta}$ is not monitored at time t ; else $R_{\alpha\beta}(t+1) = 0$ if $G_{\alpha\beta}$ was monitored at time t [7]. As the rewards are modelled as penalties, the objective of the PM problem is to find a policy for the agent to minimize the neglect time which in turn minimizes the total accumulated penalty by G , over a finite time T . The optimal policy is given as

$$\pi = \arg \max_{\pi} \sum_{t=0}^T \left[\sum_{\alpha=1}^M \sum_{\beta=1}^N R_{\alpha\beta}^{\pi}(t) \right], \quad (1)$$

where π is an optimal global joint-policy that dictates the actions of the agent in a multi-agent system, and $R_{\alpha\beta}^{\pi}$ is the reward due to following a policy π .

B. Localization for Persistent Monitoring

The grid G consists of N -agents to perform the monitoring task, with each agent being able to observe a sub-grid of size $l \times l$, (for $l < M, N$), centred at its own position, and having a communication range ρ . At every time step, a connectivity graph $\mathcal{G} = \langle \mathcal{V}, \mathcal{E} \rangle$ is generated between the agents. An edge connection e_{ij} is formed between agents i and j if they are separated by a distance within the communication range, $\text{dist}(i, j) \leq \rho$. The connectivity of any agent with an anchor agent, is checked by using Depth-First Search (DFS) algorithm. We assume that if an auxiliary agent is connected to an anchor agent, either directly or indirectly (k -hop connection), it can localize itself. This is possible because (1) all the agents are aware of their true positions with 100% belief at the beginning of the episode, and (2) the anchor agents have a high precision IMU with negligible uncertainty, so the anchor agents are always localized, hence other agents can calculate their own positions by sensing their relative position with respect to an anchor.

An agent observes $l \times l$ cells and updates the rewards $R_{\alpha\beta}(t)$ in the grid world G , that is, set $R_{\alpha\beta}(t) = 0$. We only allow the anchor and the auxiliary agents that are connected to an anchor at time t , to reset the rewards of the observed grid cells. If an auxiliary agent is unlocalized, then it cannot reset the rewards of the observed grid cells to 0. We take this constraint into account to address the problem where an unlocalized agent updates the rewards of the cells which are not actually within the observable range of its true position, but because of a low-precision IMU. The auxiliary agents

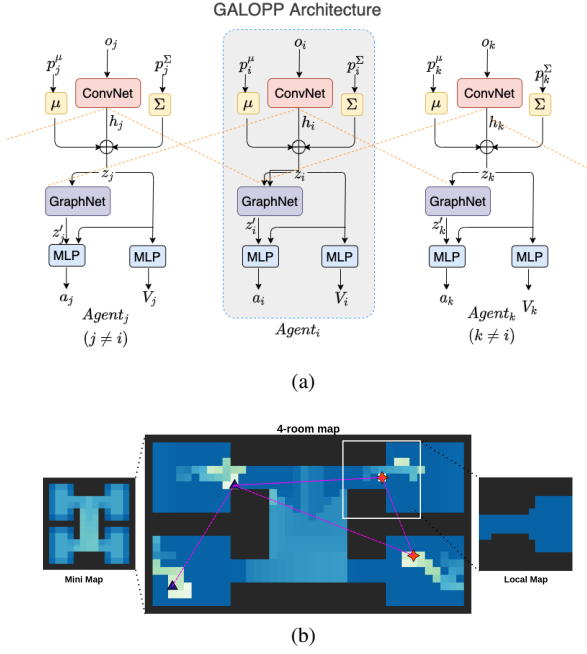


Fig. 2: (a) Schematic representation of GALOPP architecture. Each individual agent block of the architecture represents an actor-critic model. (b) The mini map is the image of the environment G , resized to $l \times l$. The local map is a $l \times l$ slice of the environment G , centered around the agent. The mini map and local map are concatenated together to form the input o_i for agent i .

use a Kalman Filter to estimate and update their positional belief when they are disconnected from an anchor and to rectify their state estimate when they reconnect to an anchor agent.

Here, solving Equation 1 does not explicitly assume that the graph network is connected at all times. Although a strict connectivity constraint increases the global positional belief of the entire team, it reduces the optimality of persistent monitoring. An intermittent connectivity of agents leads to better exploration of the area allowing more flexibility [25], [12]. The auxiliary agents once disconnected do not contribute to the net rewards obtained by the team. Since the objective is to find a policy that maximizes the rewards, the problem statement enables the agents to learn that connectivity increases the rewards and hence they should be connected. Through rewards, the connectivity constraints are indirectly implied and not hard-coded into the agent decision-making policy. The localization constraints are enabled through the connectivity graph. The Kalman filter and the subsequent mean and covariance terms have been described in detail in the supplementary material under appendix A??.

IV. GRAPH LOCALIZED PPO - GALOPP

A. Architectural overview

The GALOPP architecture, shown in Figure 2a, consists of a multi-agent actor critic model that implements Proximal Policy Optimization (PPO) [26] to determine individual agent

trajectories. The agent's observation space is the shared global reward map passed to each agent. The decentralized actors of each agent take the generated embedding from the agents to learn the policy, while a centralized critic updates the overall value function of the environment. The model uses Convolutional Neural Network (CNN) [27] to generate the individual embeddings which is then augmented with agent i 's positional mean μ_i and covariance Σ_i . This serves as the complete information z_i of the agent's current state. The Graph Attention Network (GAT) [28] enforces the relay of messages in the generated connectivity graph \mathcal{G} to ensure inter-agent communication. The model is trained end-to-end for the PM problem. The local computation involves - updating the local map, updation of the mean and covariance of the position. The central computation is the computation of the joint-policy and updating the global map. The components of the GALOPP architecture is described in the below subsections.

B. Embedding extraction and message passing

The GALOPP model takes the shared global reward values in the 2D grid as input. The observation of an agent i at time t is the set of cells that are within the sensing range (termed as local map) and also a compressed image of the current grid (termed as mini map) with the pixel values equal to the penalties accumulated by the grid cells [7]. The mini map is resized to the shape of the local map of the agent and then concatenated to form a 2-channelled image (shown in figure 2b). This forms the sensing observation input o_i for the model at time t . The CNN is used to convert the observation o_i into a low-dimensional feature vector h_i termed as the embedding vector. The positional mean μ_i and covariance matrix Σ_i of agent i , are then flattened and their elements are concatenated with h_i to generate a new information vector z_i (as represented in figure 2a).

The agents are heterogeneous agents (anchor and auxiliary) where the localization information is a parameter which is being aggregated in the graph network component of GALOPP. Since we have considered the anchor agents to be superior with respect to localization capabilities, one would typically expect a weighted aggregation of the message embeddings. The aggregated information vector of an agent is dependent on the current position in the environment, the generated message embedding, and the localization status of each neighbouring agent. Due to this, attention mechanism becomes useful to compute the attention parameters in the GALOPP model.

The GAT is used to transfer the information vector z_i to all agents within the communication graph. Agents i and j are connected if the condition $dist(i, j) < \rho$ is satisfied. The agents take in the weighted average of the embeddings of the neighbourhood agents. The attention parameter $\alpha_{i,j}$ gives an implicit weight parameter that assigns an attention value to each edge in the graph. The dynamics of the attention parameter $\alpha_{i,j}$ is given as [28],

$$\alpha_{i,j}^m = \frac{\exp(\text{LEAKYRELU}(\mathbf{a}(\mathbf{W}^m z_i, \mathbf{W}^m z_j)))}{\sum_{k \in N_i} \exp(\text{LEAKYRELU}(\mathbf{a}(\mathbf{W}^m z_i, \mathbf{W}^m z_k)))} \quad (2)$$

where, $z_i \in \mathbb{R}^F$ is the information vector of agent i ; N_i is the neighbourhood set of agent i ; \mathbf{W} is the corresponding weight parameters for the inputs; $\mathbf{a} : \mathbb{R}^F \times \mathbb{R}^F \rightarrow \mathbb{R}$ is a single-layered feedforward function known as the attention mechanism; m is the number of attention heads in the network used to stabilize the training process and to encompass complex parameter relations. LEAKYRELU is the activation function used on the output of a . After the message passing, the aggregated information vector z'_i for each agent i is given as,

$$z'_i = \frac{1}{M} \sum_{m=1}^M \left(\sum_{k \in N_i} \alpha_{i,j}^m \mathbf{W}^m z_k \right). \quad (3)$$

C. Multi-agent actor critic method using PPO

The goal of Proximal Policy Optimization (PPO) is to incorporate the trust region policy [29] constraint in the objective function. Multi-agent PPO is preferred over other policy gradient methods to avoid having large policy updates and to achieve better stability in learning in monitoring tasks. The decentralized actors in the multi-agent PPO take in the aggregated information vector z'_i and generate the corresponding action probability distribution. The centralized critic estimates the value function of the environment to influence the policy of the individual actors. The shared reward for all agents is defined in Equation (1).

The multi-agent PPO algorithm [7] is modified for GALOPP. For a defined episode length T , the agent interacts with the environment to generate and collect the trajectory values in the form of states, actions, and rewards $\{s_i, a_i, \mathcal{R}_i\}$. The stored values are then sampled iteratively to update the action probabilities and to fit the value function through back-propagation. The PPO gradient expression is the expected product of the advantage estimate function and the log probabilities.

$$\nabla J(\theta) = \mathbb{E}_{\pi_\theta} [\nabla_\theta \log \pi_\theta(a_i | s_i) \hat{A}_i] \quad (4)$$

where the advantage estimate function \hat{A}_i is defined as the difference between the discounted sum of rewards ($Q_i(s_i, a_i)$) and the state value estimate ($V_i(s_i)$) as $\hat{A}_i(s_i, a_i) = Q_i(s_i, a_i) - V_i(s_i)$. The clipped surrogate objective function for a single PPO agent i is given by

$$L_i^{CLIP}(\theta) = \hat{\mathbb{E}}_t [\min(r_t(\theta) \hat{A}_t^i, \text{clip}(r_t(\theta), 1 - \epsilon, 1 + \epsilon) \hat{A}_t^i)],$$

where, $r_t(\theta)$ is the ratio of the action probability in the current policy to the action probability in the previous policy distribution for trainable parameter θ . The *clip* function clips the probability ratio $r_t(\theta)$ to the trust-region interval $[1 - \epsilon, 1 + \epsilon]$. The modified multi-agent PPO objective function to be minimized in the GALOPP network is given as

$$L(\theta) = \frac{1}{m} \sum_m \left(\frac{1}{N} \sum_{i=1}^N (L_i^{CLIP}(\theta)) \right) \quad (5)$$

where, N is the total number of agents and m is the mini-batch size.

V. EXPERIMENTS AND ANALYSIS

To evaluate the performance of GALOPP, we custom-built three environments: 2-room map, 4-room map and a random map as shown in Figure 3. The agents have a sensing range of 15×15 units. We use the accumulated penalty metric for the evaluation and also evaluate the effect of communication range on the performance. Due to space restriction, we provide some key results.

Training: For the 2-room case, the training is carried out for 30000 episodes, while its 50000 episodes for the 4-room map case with each episode length $T = 1000$ time steps. The penalties in the grid cells are updated with decay-rate of $\Delta_{\alpha\beta} = 1, \forall(\alpha, \beta)$. The maximum penalty a cell can have is $R_{max} = 400$. The total reward at time t is defined as $\mathcal{R}(t) = \sum_{\alpha, \beta} R_{\alpha\beta}(t)$. For every training episode, the agents are initialized randomly in the environment but localized.

The GALOPP architecture input at time t is the image representing the state of the grid G^t , resized to a 15×15 image using OpenCV's INTER_AREA interpolation method, and concatenated with the local visibility map of the agent, forming a 15×15 2-channeled image. The action space includes 5 possible actions: front, back, left, right and stay. Each action enables the agent to move by one pixel, respectively. For testing the learned trajectories, we evaluate it for 100 episodes, each episode for $T = 1000$ time steps, in their respective environments. The reward for test episode τ is denoted by \mathcal{R}_{ep}^τ and is the summation of the reward at each time step t of the episode i.e. $\mathcal{R}_{ep}^\tau = \sum_{t=1}^T \mathcal{R}(t)$ and the final reward \mathcal{R}_{avg} after $n = 100$ episodes is calculated by averaging the rewards of each episode i.e. $\mathcal{R}_{avg} = \sum_{\tau=1}^n \mathcal{R}_{ep}^\tau / n$. The \mathcal{R}_{avg} is used to evaluate the performance of the model.

Evaluation: For the 2-room map, 3 agents (1 anchor and 2 auxiliary agents) with comm range 20 are deployed. For the 4-room map we deploy 4 agents (2 anchor and 2 auxiliary agents) with 20 units comm range. And, for the open map, we use total 4 agents (2 anchor and auxiliary agents). Figure 4a, 4b, and 4c shows the training curves for all the mentioned environments.

The simulation parameters and the computer architecture used have been mentioned in appendix B?? of the supplementary material.

Comparing the performance of GALOPP with non-RL

baselines: Due to the localization constraints in the PM problem, the motion of the anchor agents and the auxiliary agents become coupled. Thus generating deterministic motion strategies for these heterogeneous agents becomes highly complex. We compare the performance of GALOPP with 3 non-RL baselines: Random Search (RS), Random Search with Ensured Communication (RSEC) and Greedy Decentralized Search (GDCS). In Random Search, each agent randomly chooses from the available actions uniformly, without caring if an auxiliary agent gets unlocalized. In RSEC, every agent chooses a random action and checks if taking that action will lead to its unlocalization or the unlocalization of any other agent. If so, then it randomly chooses from the remaining actions and so on until it finds

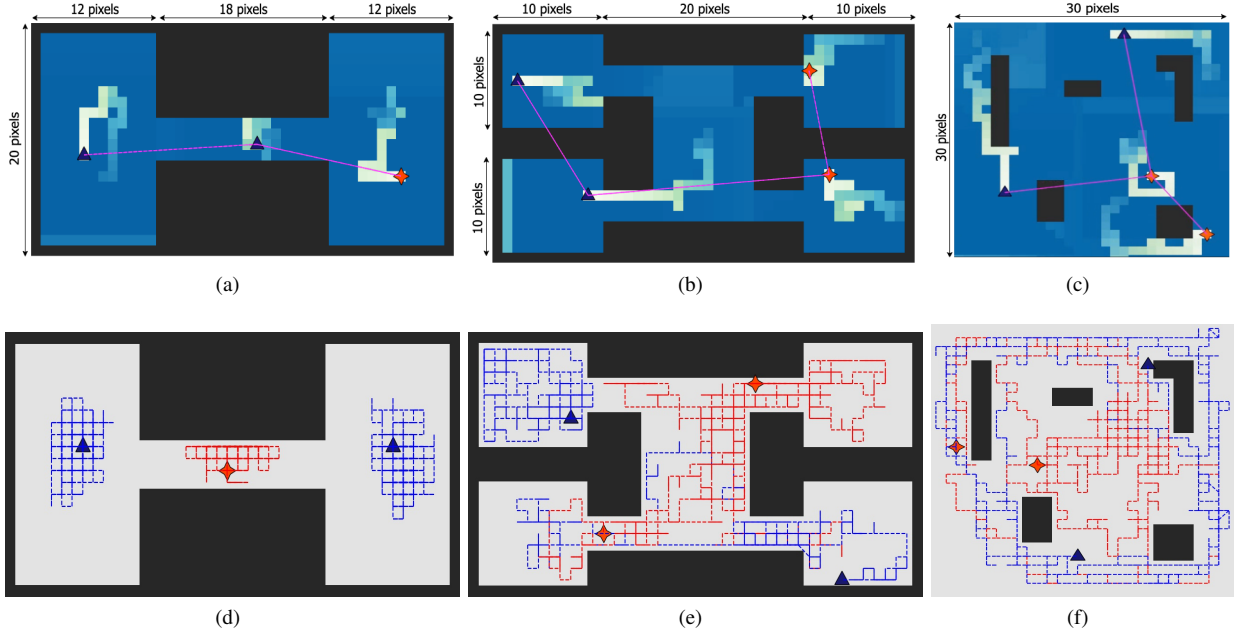


Fig. 3: The (a) 2-room (b) 4-room, and (c) open-room maps. The agents cannot move into black pixels, while the non-black regions needs to be persistently monitored. As the anchor agents (red stars), and auxiliary agents (dark blue triangles) monitor, their trajectory is shown as the fading white trails for the last 30 steps. Communication range between the agents is shown in red lines. (d)-(e) The trajectories of the anchor and auxiliary agents while monitoring.

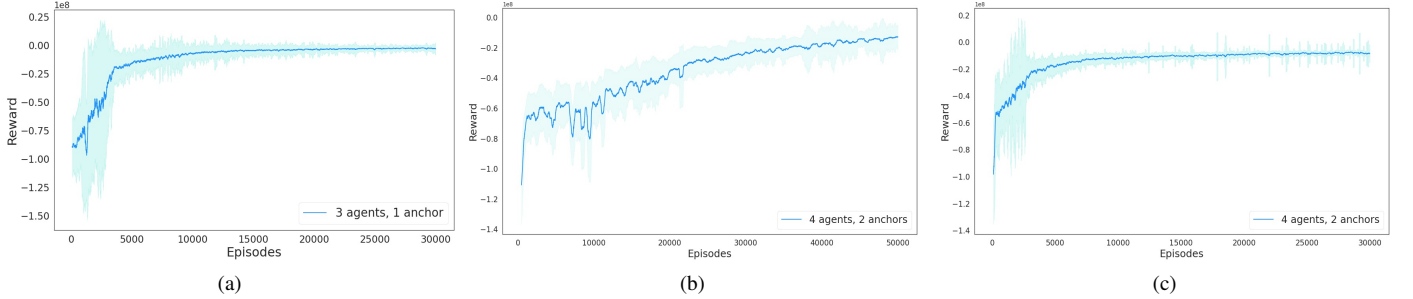


Fig. 4: Comparison of the training curves (rolling average of 100 episodes and \pm std error band) for the (a) 2-room, (b) 4-room, and (c) open-room environments.

an action that won't unlocalize itself or any other agent.

In GDCS, agents act independently and greedily. Given that an agent i has an $l \times l$ visibility range, is currently located at position (x, y) and G' defines the set of grid cells that fall on the unobstructed line of sight of agent i , we define: $\mathbb{G} = \{G_{\alpha\beta} \in G' | \alpha \in [x - (\frac{l}{2} + 1), \dots, x + (\frac{l}{2} + 1)], \beta \in [y - (\frac{l}{2} + 1), \dots, y + (\frac{l}{2} + 1)], (\alpha, \beta) \neq (x \pm (\frac{l}{2} + 1), y \pm (\frac{l}{2} + 1))\}$, which is a set of cells that are just one step beyond agent i 's visibility range. A_i chooses an action that takes it towards the cell with the maximum penalty in \mathbb{G} . If all the grid cells in \mathbb{G} have the same penalty, then A_i chooses a random action. GDCS does not impose the communication constraint while taking an action.

Figure ?? and ?? compare the performance of our architecture with the baselines. In the 2-room map case, Figure ??, GDCS and GALOPP always outperform the random base-

lines (RS and RSEC) by a significant margin. But coming to GDCS, its performance is close to that of GALOPP, with certain instances where it performs better than our algorithm (hence the high standard deviation on the GDCS bars in Figure ??). Our tests revealed that the GDCS algorithm is highly susceptible to the initialization positions of the agents. GDCS only performs well when the agents are initialized in a manner when most of the cells fall within the unobstructed line of sight of the agents (this happens mainly when the agents are initialized near to or in the central corridor region of the 2-room map. But when the agents are initialized in an unfavourable location like in corners of one of the rooms, then GDCS leads to a situation where the agents are stuck leading to sub-optimal trajectory that propagates to some of the grid cells reaching R_{max} in their penalties.

However, GALOPP can adapt to random initialization

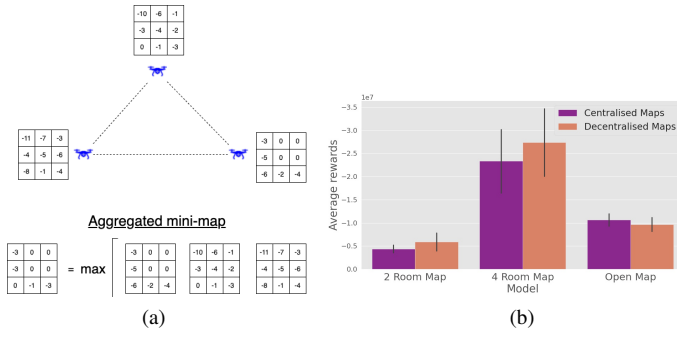


Fig. 5: Overview and performance of decentralized maps vs centralized maps

positions and plan the trajectories accordingly. In the 2-room map we notice that our algorithm ends up with the agents in a formation where two of the agents position themselves in the 2 rooms while one agent monitors the corridor. This can be seen in Figure 3a where the faded cells show the trajectory followed by the agents.

Figure ?? compares the performance of GALOPP in the 4-room map. We notice that in this case, the GDCS is outperformed by the random baselines and GALOPP. The poor performance of the GDCS algorithm can be attributed to the narrow passages that lead to the individual rooms. This obstructs the view of the agents into the grid cells within the room, hence leaving a subset of rooms unmonitored. This comes to show that GDCS does not adapt well to complex environment apart from being highly dependent on the agents' initialization locations. GALOPP performs better than the random baselines as well, with a significant improvement in performance and the ability to adapt to complex environments. We see that even in this case, our algorithm learns a trajectory to maintain a formation where each of the 4 agents, monitor a room and they intermittently exit the room to monitor the central corridor region (shown in Figure 3b).

Effect of varying communication range: We analyze the effect of changing the communication range ρ to the overall performance. Initially, for the 2-room map communication ranges from 15 to 25 units (pixels) are considered, while in the 4-room map ρ from 20 to 40 units are considered.

In the 2-room map (Figure ??) we notice that the model with $\rho = 15$ performs worse while the models with $\rho = 20$ and $\rho = 25$ are almost equal in their performance. On the other hand, for the 4-room map (Figure ??) we notice consistently similar performance for all the communication ranges. The figure also shows that beyond a certain minimum ρ , GALOPP performs almost identically similar with increasing communication range. This is also intuitive because as ρ increases, it will only facilitate the localization of the auxiliary agents at further distances from the anchor agents where as the optimum policy would not require it to go to such large distances.

Figure ?? shows the average percentage of time an agent is unlocalized during an episode. This is calculated by $U =$

$\sum_{i=1}^K U_i / K$ where K is the total number auxiliary agents and U_i the total unlocalization time for each auxiliary agent in an episode. This is then repeated for all the 100 episodes and averaged over them. In case of the 2-room map we see high unlocalization times for $\rho = 15$ followed by a drop for $\rho = 20$ and then a rise again when $\rho = 25$. Even though the unlocalization times for $\rho = 25$ are high, Figure ?? shows that it performs similar to the model with $\rho = 20$. This suggests the emergence of policies that might not require localization of the auxiliary agents during the entire episode while still performing optimally. For the 4-room map on the other hand (Figure ??), there is a steady drop in the unlocalization time as the comm range increases and its unlocalization time is far less when compared to the same comm range in the 2-room map. This is because the 4-room map had 2 anchor agents which lead to higher localization time for the auxiliary agents, as opposed to the 2-room map that only had 1 anchor agent.

A. Decentralized maps

Having a fully-shared global map information to all the agents requires having a centralized map computation. A fully centralized map hampers the scalability of the system to a larger environment. To circumvent this, we equip each agent with a separate individual copy of the global map. Each agent continues to update the copy of their global map, and the monitoring awareness is updated through inter-agent connectivity. Figure 5a shows a schematic representation of the decentralized map updation. For a network graph, the connected agents compare and aggregate the global map at each time-step by taking the element-wise maximum for each grid cell $G_{\alpha\beta}$ in the environment. In figure 5b, we compare the performance of the decentralized map with the centralized map for the 2-room, 4-room, and open-room map using the agent configuration mentioned in section V.

VI. CONCLUSION

This paper developed a MADRL with graph attention based approach – GALOPP for persistently monitoring a bounded region taking the communication, sensing and localization constraints into account. The agents learnt the environment and modified their trajectories to satisfy the conflicting objectives of coverage and meeting localization constraints based on the environmental conditions. The experiments show that the agents using GALOPP outperformed the greedy and random baseline strategies. This work can be further work extended to study its scalability to larger number of agents, robustness to varying environments and resilience in case of agent failures.

REFERENCES

- [1] J. Yu, S. Karaman, and D. Rus, "Persistent monitoring of events with stochastic arrivals at multiple stations," *IEEE Transactions on Robotics*, vol. 31, no. 3, pp. 521–535, 2015.
- [2] P. Tokekar and V. Kumar, "Visibility-based persistent monitoring with robot teams," in *IEEE/RSJ International Conference on Intelligent Robots and Systems*, 2015, pp. 3387–3394.

- [3] S. L. Smith, M. Schwager, and D. Rus, "Persistent monitoring of changing environments using a robot with limited range sensing," in *IEEE International Conference on Robotics and Automation*, 2011, pp. 5448–5455.
- [4] S. K. K. Hari, S. Rathinam, S. Darbha, K. Kalyanam, S. G. Manyam, and D. Casbeer, "The generalized persistent monitoring problem," in *American Control Conference*, 2019, pp. 2783–2788.
- [5] X. Lin and C. G. Cassandras, "An optimal control approach to the multi-agent persistent monitoring problem in two-dimensional spaces," *IEEE Transactions on Automatic Control*, vol. 60, no. 6, pp. 1659–1664, 2014.
- [6] S. K. K. Hari, S. Rathinam, S. Darbha, K. Kalyanam, S. G. Manyam, and D. Casbeer, "Optimal uav route planning for persistent monitoring missions," *IEEE Transactions on Robotics*, vol. 37, no. 2, 2021.
- [7] J. Chen, A. Baskaran, Z. Zhang, and P. Tokekar, "Multi-agent reinforcement learning for persistent monitoring," *arXiv preprint arXiv:2011.01129*, 2020.
- [8] Honeywell, "Hg1700." [Online]. Available: <https://aerospace.honeywell.com/en/learn/products/sensors/hg1700-inertial-measurement-unit>
- [9] J. Zhu and S. S. Kia, "Cooperative localization under limited connectivity," *IEEE Transactions on Robotics*, vol. 35, no. 6, pp. 1523–1530, 2019.
- [10] J. Liu, J. Pu, L. Sun, and Y. Zhang, "Multi-robot cooperative localization with range-only measurement by uwb," in *Chinese Automation Congress*. IEEE, 2018, pp. 2809–2813.
- [11] R. Sharma, R. W. Beard, C. N. Taylor, and S. Quebe, "Graph-based observability analysis of bearing-only cooperative localization," *IEEE Transactions on Robotics*, vol. 28, no. 2, pp. 522–529, 2011.
- [12] R. Khodayi-mehr, Y. Kantaros, and M. M. Zavlanos, "Distributed state estimation using intermittently connected robot networks," *IEEE Transactions on Robotics*, vol. 35, no. 3, pp. 709–724, 2019.
- [13] J. O'Rourke *et al.*, *Art gallery theorems and algorithms*. Oxford University Press Oxford, 1987, vol. 57.
- [14] X. Tan, "Fast computation of shortest watchman routes in simple polygons," *Information Processing Letters*, vol. 77, no. 1, pp. 27–33, 2001.
- [15] E. Galceran and M. Carreras, "A survey on coverage path planning for robotics," *Robotics and Autonomous systems*, vol. 61, no. 12, pp. 1258–1276, 2013.
- [16] J. Blumenkamp and A. Prorok, "The emergence of adversarial communication in multi-agent reinforcement learning," *Conference on Robot Learning*, Cambridge, MA, USA, 2020.
- [17] S. Omidshafiei, J. Pazis, C. Amato, J. P. How, and J. Vian, "Deep decentralized multi-task multi-agent reinforcement learning under partial observability," in *International Conference on Machine Learning*, Sydney, Australia, 2017, pp. 2681–2690.
- [18] D. Maravall, J. de Lope, and R. Domínguez, "Coordination of communication in robot teams by reinforcement learning," *Robotics and Autonomous Systems*, vol. 61, no. 7, pp. 661–666, 2013.
- [19] Q. Li, F. Gama, A. Ribeiro, and A. Prorok, "Graph neural networks for decentralized multi-robot path planning," *IEEE International Conference on Intelligent Robots and Systems*, 2019.
- [20] R. Shah, Y. Jiang, J. Hart, and P. Stone, "Deep r-learning for continual area sweeping," in *IEEE/RSJ International Conference on Intelligent Robots and Systems (IROS)*, Las Vegas, 2020, pp. 5542–5547.
- [21] Q. Li, W. Lin, Z. Liu, and A. Prorok, "Message-aware graph attention networks for large-scale multi-robot path planning," *IEEE Robotics and Automation Letters*, vol. 6, no. 3, pp. 5533–5540, 2021.
- [22] R. Lowe, Y. Wu, A. Tamar, J. Harb, P. Abbeel, and I. Mordatch, "Multi-agent actor-critic for mixed cooperative-competitive environments," in *Proceedings of the 31st International Conference on Neural Information Processing Systems*, Long Beach, California, USA, 2017, p. 6382–6393.
- [23] A. I. Mourikis and S. I. Roumeliotis, "Performance analysis of multirobot cooperative localization," *IEEE Transactions on robotics*, vol. 22, no. 4, pp. 666–681, 2006.
- [24] L. Du, L. Chen, X. Hou, and Y. Chen, "Cooperative vehicle localization base on extended kalman filter in intelligent transportation system," in *Wireless and Optical Communications Conference*. IEEE, 2019, pp. 1–5.
- [25] F. Klaesson, P. Nilsson, A. D. Ames, and R. M. Murray, "Intermittent connectivity for exploration in communication-constrained multi-agent systems," in *ACM/IEEE International Conference on Cyber-Physical Systems*, 2020, pp. 196–205.
- [26] J. Schulman, F. Wolski, P. Dhariwal, A. Radford, and O. Klimov, "Proximal policy optimization algorithms," *arXiv preprint arXiv:1707.06347*, 2017.
- [27] Y. LeCun, Y. Bengio *et al.*, "Convolutional networks for images, speech, and time series," *The handbook of brain theory and neural networks*, vol. 3361, no. 10, p. 1995, 1995.
- [28] P. Veličković, G. Cucurull, A. Casanova, A. Romero, P. Liò, and Y. Bengio, "Graph Attention Networks," *International Conference on Learning Representations*, Vancouver, Canada, 2018.
- [29] J. Schulman, S. Levine, P. Abbeel, M. Jordan, and P. Moritz, "Trust region policy optimization," in *International conference on machine learning*. PMLR, Lille, France, 2015, pp. 1889–1897.